THE JOURNAL OF PHYSICAL CHEMISTRY A

ARTICLE

pubs.acs.org/JPCA

Solid-State Thermochromism and Phase Transitions of Charge Transfer 1,3-Diamino-4,6-dinitrobenzene Dyes

Jong Hoon Lee,[†] Panče Naumov,[*,‡] Ihn Hee Chung,[†] and Sang Cheol Lee[*,†]

[†]School of Advanced Materials and System Engineering, Kumoh National Institute of Technology, Gumi 730−701, Korea

[‡]Department of Material and Life Science, Graduate School of Engineering, Osaka University, 2−1 Yamada-oka, Suita, Osaka 565−0871, Japan

Supporting Information

ABSTRACT: The lower 1,3-bis(hydroxyalkylamino) homologues of the strong intramolecular X-type charge transfer (CT) system 1,3-diamino-4,6-dinitrobenzene (DADNB) exhibit reversible color change in the solid state from yellow at room temperature (RT) to orange and red at high temperature (HT). To investigate the structural prerequisites for occurrence of this phenomenon, we prepared 10 new derivatives of DADNB where the hydroxyalkyl arms at the amino groups were replaced with substituents having different electronic and steric profiles. Two of the new materials exhibit sharp and reversible thermochromic change in the solid state: when heated, the bis(aminoethyl) derivative (DADNB-1) undergoes color change from orange-red to brown, while one of the three polymorphs of the bisphenyl product (DADNB-2) changes its color from red to yellow. The physicochemical analysis and the crystal structures of seven of these compounds, one of which is trimorphic, confirmed that both phenomena are due to solid−solid phase transitions. The brown high-temperature phase of DADNB-1 presents the first example where the absorption is shifted beyond the red region. Form C of DADNB-2 is the first material of this group that exhibits "negative" thermochromism, where the high-temperature phase absorbs at lower wavelength than the low-temperature one. The results demonstrate the potentials of these simple and easily accessible organic molecular materials for thermal switching of the optical properties by utility of intermolecular interactions to modulate the intramolecular CT.

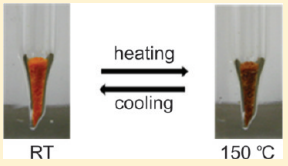

1. INTRODUCTION

The ability of certain materials to undergo a reversible change of their color is of great importance for analytical, industrial and other applications.[1] Color change can be induced, for instance, by action on the material with heat (thermochromism), light (photochromism), pressure (piezochromism), electricity (electrochromism), solvent (solvatochromism), or by addition of acids/bases/salts (halochromism). Of these, the materials that exhibit thermochromism in the solid state, typically represented by some spiroheterocyclic compounds (e.g., spiropyrans and spirooxazines),[2] Schiff bases (e.g, salicylideneanilines),[3] and polycyclic overcrowded enes (overcrowded ethylenes),[4] are an important research theme, not only because of the appealing thermal visual effects that are oftentimes employed for demonstrative and educational purposes, but also because of their potentials for applications as "smart materials" for fabrication of temperature-sensitive elements: light filters, thermal indicators, and optical switching and imaging systems.[5] The solid-state thermochromic effects of organic compounds, however, are limited to a few processes, and most of the newly reported compounds belong to some of these families, typically *cis*−*trans* isomerizations, pericyclic reactions, or group/hydrogen transfer.[2−4]

Recently, we reported and characterized several 1,3-bis(hydroxyalkylamino)-4,6-dinitrobenzenes (BDB*n* in Scheme 1, $n = 2-5$), a new group of charge transfer (CT) thermochromic solids that are homologous to the prototypic X-type organic CT system 1,3-diamino-4,6-dinitrobenzene (DADNB, Scheme 1).[6−8] When heated, crystals or powders of some BDB*n* polymorphs[9] exhibit dramatic color change from bright yellow to red. For $n = 2-4$, the color change of heated crystals proceeds in two thermal regimes: *gradual* change from yellow to orange, a process that was attributed to increased $\pi-\pi$ separation between the aromatic rings and enhanced intramolecular CT on the expense of the intermolecular CT, followed by a *sharp* color change from orange to red, which based on the IR spectra had been previously tentatively assigned[6,7] to intramolecular proton transfer and formation of a monoaci-nitro product (it should be noted, however, that there is no direct evidence yet to substantiate the latter mechanism, because degradation of the crystallinity during the phase transition has burdened structural determination of the product phases). The color change is reversible, and the yellow color of the BDB*n* crystals is recovered on cooling with a kinetics that is determined by the length of the alkyl arm *n* and the actual crystal form.

To investigate the role of the substitution at the amino functionality of DADNB on the BDB*n*-type thermochromism, as well as to investigate whether this property is a more general phenomenon characteristic for similar CT compounds, in this work we prepared, characterized and studied the thermal behavior of ten new 1,3-bis(alkylamino)-4,6-dinitrobenzenes

Received: June 20, 2011
Revised: July 15, 2011
Published: July 26, 2011

dx.doi.org/10.1021/jp205793b | *J. Phys. Chem. A* 2011, 115, 10087–10096

Scheme 1. Chemical Structures of 1,3-Diamino-4,6-dinitrobenzene (DADNB), 1,3-Bis(hydroxyalkylamino)-4,6-dinitrobenzenes (BDB*n*, *n* = 2−5) and the DADNB Derivatives Studied in this Work (DADNB-*n*, *n* = 1−10)

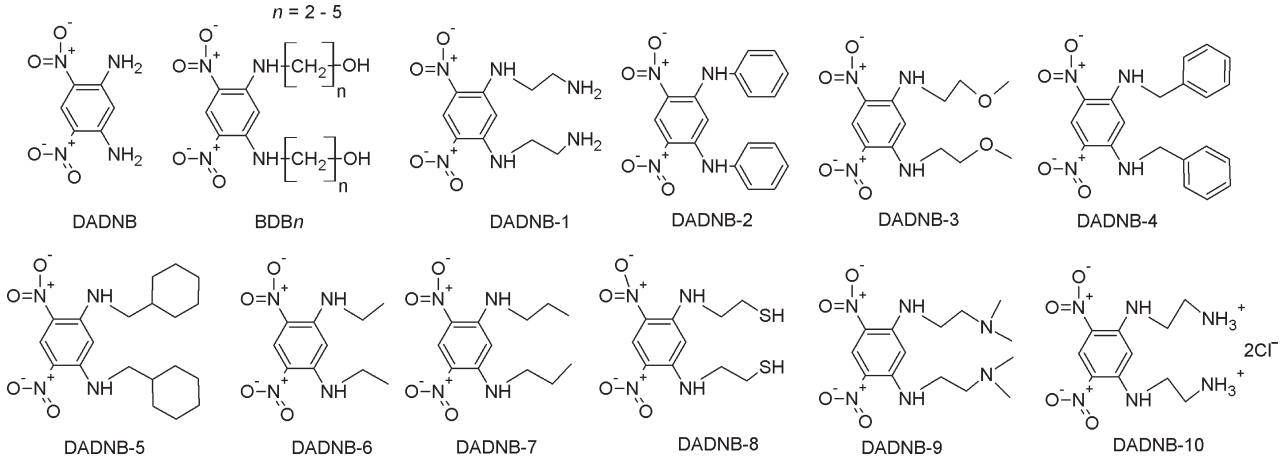

(DADNB-*n*, *n* = 1−10 in Scheme 1). In these structures, the hydroxyalkyl arms at the amino groups were symmetrically substituted with a variety of substituents which were selected so as to reflect different steric and electronic requirements. With two of these materials, those having aminoethyl (DADNB-1) and phenyl (DADNB-2) substituents, we observed reversible color change in the solid state. From DADNB-2 we succeeded to isolate and structurally characterize three polymorphs with different physical and structural properties, and we established the modes of their interconversion in the solid state. Notably, contrary to the BDB*n* compounds, where the heating results in color change from yellow to orange and red, one of these materials showed change of color to brown, which indicates strong effects of the CT and decrease of the excited-state energy. In the case of the other compound, we observed a "negative" thermochromism, where the room temperature (RT) form is red and the high temperature (HT) phase is yellow, which is a yet unobserved case in this CT system.

2. EXPERIMENTAL SECTION

2.1. Synthetic Procedures and Analytical Data. *1,5-Bis-(aminoethylamino)-2,4-dinitrobenzene (DADNB-1).* A total of 50 g (0.34 mol) *m*-dichlorobenzene was reacted with 70 g (0.693 mol) KNO_3 in concentrated H_2SO_4 solution (250 mL) at 130 °C for 1 h. The reaction product, 2,6-dichloro-3,5-dinitrobenzene, was filtered, dissolved in boiling 95% ethanol (1000 mL) and recrystallized at 0 °C. 24 mL ethylenediamine in ethanol (50 mL) were slowly added to 55 g 2,6-dichloro-3,5-dinitrobenzene (0.211 mol) in the course of 0.5 h, and the mixture was stirred 5 h to complete the reaction. The solid product (DADNB-1) was filtrated, washed with water, and recrystallized from ethanol. FT-IR (cm^{-1}): 3388, 3328 (N−H stretch), 2920, 2835 (aliphatic C−H stretch), 1573, 1403 (NO_2), 1541, 1451 (aromatic C=C stretch). ^1H NMR (200 MHz, DMSO-d_6): δ 2.84 (t, 4H), 3.22 (s, 4H), 3.33 (t, 4H), 5.86 (s, 1H), 8.63 (s, 2H), 8.96 (s, 1H).

1,5-Bis(phenylamino)-2,4-dinitrobenzene (DADNB-2). In a typical procedure for the preparation of these compounds, 2,6-dichloro-3,5-dinitrobenzene (0.59 g, 0.0025 mol) in ethanol (50 mL) was added dropwise to aniline (0.93 g, 0.0025 mol) in ethanol (50 mL) and the solution was stirred 4 h to complete the reaction. The product was filtered and purified by recrystallization from ethanol. Analytical data: FT-IR (cm^{-1}): 3324 (N−H stretch), 3123 (aromatic C−C stretch), 1567, 1410 (NO_2), 1534, 1455 (aromatic C=C stretch). ^1H NMR (200 MHz, acetone-d_6): δ 6.56 (s, 1H), 7.23 (t, 2H), 7.34 (d, 4H), 7.42 (t, 4H), 9.20 (s, 1H), 9.78 (s, 2H).

1,5-Bis(2-methoxyethylamino)-2,4-dinitrobenzene (DADNB-3). FT-IR (cm^{-1}): 3363 (N−H stretch), 2920, 2835 (aliphatic C−H stretch), 1577, 1407 (NO_2), 1541, 1451 (aromatic C=C stretch), 1255 (C−N stretch), 1150 (C−O strech). ^1H NMR (200 MHz, acetone-d_6): δ 3.39 (s, 6H), 3.58−3.65 (m, 4H), 3.69−3.74 (m, 4H), 6.11 (s, 1H), 8.51 (s, 2H), 9.10 (s, 1H).

1,5-Bis(benzylamino)-2,4-dinitrobenzene (DADNB-4). FT-IR (cm^{-1}): 3365 (N−H stretch), 3089 (aromatic C−C stretch), 1575, 1409 (NO_2), 1541, 1452 (aromatic C=C stretch), 1222 (C−N stretch). ^1H NMR (200 MHz, acetone-d_6): δ 4.55 (d, 4H), 5.91 (s, 1H), 7.24−7.36 (m, 10H), 8.88 (s, 2H), 9.12 (s, 1H).

1,5-Bis(cyclohexanemethylamino)-2,4-dinitrobenzene (DADNB-5). FT-IR (cm^{-1}): 3363 (N−H stretch), 3108 (aromatic C−C stretch), 2925, 2850 (sp^3 C−H stretch), 1580, 1409 (NO_2), 1537, 1453 (aromatic C=C stretch), 1241 (C−N stretch). ^1H NMR (200 MHz, chloroform-*d*): δ 0.85−1.41 (m, 20H), 3.11 (t, 4H), 5.61 (s, 1H), 8.42 (s,2H), 9.24 (s, 1H).

1,5-Bis(ethylamino)-2,4-dinitrobenzene (DADBN-6). FT-IR (cm^{-1}): 3376 (N−H stretch), 3100 (aromatic C−C stretch), 2984 (aliphatic C−H stretch), 1540, 1347 (NO_2), 1540, 1451 (aromatic C=C stretch), 1241 (C−N stretch). ^1H NMR (200 MHz, acetone-d_6): δ 1.37 (t, 6H), 3.60−3.70 (m, 4H), 7.31 (s, 1H), 8.64 (s, 2H), 8.96 (s, 1H).

1,5-Bis(propylamino)-2,4-dinitrobenzene (DADNB-7). FT-IR (cm^{-1}): 3345 (N−H stretch), 3105 (aromatic C−C stretch), 2963, 2875 (aliphatic C−H stretch), 1583, 1348 (NO_2), 1544, 1348 (aromatic C=C stretch), 1258 (C−N stretch). ^1H NMR (200 MHz, chloroform-*d*): δ 1.08 (t, 6H), 1.71−1.89 (m, 4H), 3.19−3.29 (m, 4H), 5.53 (s, 1H), 8.32 (s, 2H), 9.22 (s, 1H).

1,5-Bis(N,N-dimethylethylamino)-2,4-dinitrobenzene (DADNB-9). FT-IR (cm^{-1}): 3350 (N−H stretch), 2947, 2823, 2765 (aliphatic C−H stretch), 1577, 1407 (NO_2), 1542, 1467 (aromatic C=C

stretch), 1212 (C−N stretch). ^{1}H NMR (200 MHz, chloroform-*d*): δ 2.31 (s, 12H), 2.65 (t, 4H), 3.28−3.36 (m, 4H), 5.63 (s, 1H), 8.68 (s, 2H), 9.23 (s, 1H).

1,5-Bis(thiolethylamino)-2,4-dinitrobenzene (DADNB-8). FT-IR (cm^{-1}): 3345 (N−H stretch), 3094 (aromatic C−C stretch), 1575, 1413 (NO_2), 1534, 1456 (aromatic C=C stretch), 1218 (C−N stretch).

Hydrochloride Salt of 1,5-Bis(aminoethylamino)-2,4-dinitrobenzene (DADNB-10). To a mixture of 1,5-bis(aminoethylamino)-2,4-dinitrobenzene in water, HCl was added to pH 1 and the solution was diluted with 1.5 L water. The product was filtered, washed with water, and purified by recrystallization from water.

2.2. Physicochemical Characterization. The thermally induced color change of DADNB-1 and DADNB-2 were recorded with digital camera and their thermal properties were analyzed with differential scanning calorimeter (DSC 200 F3, Netzch) at a heating rate of 10 °C/min. A pyrogram of DADNB-1 was obtained with a thermogravimetric analyzer (TGA Q-500, TA) at a heating rate of 2 °C/min. For powders sandwiched between two glass plates, the UV−vis spectra were recorded with UV−visible reflectance spectrophotometer (ColorEye 3100, Gretag Macbeth). The visible spectrum was obtained by measuring spectral reflectance (R) and by applying the Kubelka−Munk equation: $K/S = [(1 - R)^2]/(2R)$, where K is the absorption coefficient and S is the scattering coefficient. The measurements at high temperatures were performed under nitrogen atmosphere in order to prevent thermal degradation. The infrared spectra of powdered samples in KBr pellets were recorded with FT-IR spectrometer (FT-IR 2000, Perkin-Elmer) equipped with a custom-designed temperature-controlling accessory. The ^{1}H NMR spectra (DMSO-d_6) were recorded with FT-NMR spectrometer (AMX500, Bruker, the spectra are deposited as Supporting Information, SI).

2.3. X-ray Diffraction. The temperature-dependent powder X-ray diffraction (XRD) patterns were recorded in the 2θ range 5−40° (Cu Kα radiation) at a scanning rate of 2°/min by using wide-angle X-ray diffractometer (D/MAX-2500, Rigaku) equipped with a general area detector and heating accessory. To investigate the recovery rate of the crystal-to-crystal phase transition at different fixed temperatures, the samples were kept in an oven for 10 min at 150 °C, and the changes in the diffraction with time were recorded at constant temperatures (30, 40, or 50 °C). Single crystals of sufficient quality were obtained by slow evaporation from ethanol solutions, except for form A of DADNB-2, which was grown from acetone−ethanol mixture (crystals grown from ethanol had identical structure). The single crystal XRD data were collected in ω and/or φ-scan mode with APEX2 diffractometer (Bruker AXS),[10] using Mo Kα X-rays obtained from a rotating anode source, monochromated by confocal multilayer X-ray mirror, and using CCD as area detector. The integrated and scaled data[10] were empirically corrected for absorption effects with SADABS.[11] The structures were solved by using direct methods[12] and refined on F_o^2 with SHELXL.[13] All nonhydrogen atoms were treated anisotropically, and all aromatic hydrogen atoms were included as riding bodies.

One of the propyl groups in DADNB-7 is disordered over two positions. The disorder was treated by constraining the 1,2-distances to the respective values in the other (ordered) propyl groups (C−N = 1.45 Å, C−C = 1.50 Å), and using equal isotropic thermal displacement parameters for the components of the respective terminal methyl group. One of two methylene groups of the major component was assigned anisotropic, while those of the minor component were assigned isotropic thermal parameters. The two components of the disordered alkyl chain refined to 75.7 and 24.3%. This disorder of DADNB-7 is very similar to that observed in the "open form" (form B) of BDB2,[8] where the alkyl arm which is nonplanar with the benzene ring is disordered over two positions (see Figure S13 in the SI). Similar disorder was also observed in one of the four independent molecules of phase D of BDB2.[8] The disorder in these crystals is likely to be a consequence of the similar substituents of identical length, 1-propyl in DADNB-7 and 3-hydroxyethyl in BDB2. From the specific structural features of the other structures, in DADNB-5 the molecule sits on a mirror plane so that the asymmetric unit contains only half of the molecule, and one of the cylohexyl rings is disordered over two positions. The 1,2 C−C distances were constrained to 1.5 Å. All nonhydrogen atoms, including the disordered ones, were assigned anisotropic displacement parameters.

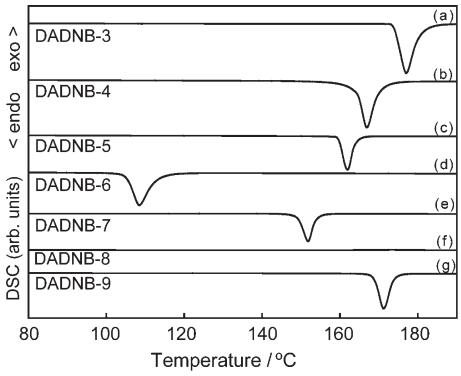

Figure 1. DSC curves, recorded by heating at 10 °C/min, of (a) 1,5-bis(2-methoxyethylamino)-2,4-dinitrobenzene (DADNB-3), m.p. 177 °C; (b) 1,5-bis(benzylamino)-2,4-dinitrobenzene (DADNB-4), m.p. 166.7 °C; (c) 1,5-bis(cyclohexanemethylamino)-2,4-dinitrobenzene (DADNB-5), m.p. 162.2 °C; (d) 1,5-bis(ethylamino)-2,4-dinitrobenzene (DADNB-6), m.p. 108.3 °C; (e) 1,5-bis(propylamino)-2,4-dinitrobenzene (DADNB-7), m.p. 152 °C; (f) 1,5-bis(thiolethylamino)-2,4-dinitrobenzene (DADNB-8); and (g) 1,5-bis(*N*,*N*-dimethylethylamino)-2,4-dinitrobenzene (DADNB-9), m.p. 171 °C. DADNB-10 (not shown here) decomposes at 300 °C (see Figure S9 in the SI).

3. RESULTS AND DISCUSSION

3.1. Thermal Characterization and Crystal Structures of DADNB-*n* (*n* = 3−10). Except for DADNB-8, which always appeared as amorphous powder, the products DADNB-*n* (Scheme 1) were readily obtained in pure state as gram-amount quantities. Except DADNB-1 and DADNB-2, which are orange or orange-yellow crystalline solids, the compounds separate from ethanol as vividly yellow crystals. All materials were air-stable. The chemical structures of the products were confirmed by ^{1}H NMR and FT-IR spectroscopy (plots of the spectra are deposited as Figures S1−S8 in the SI).

The DSC curves of DADNB-*n*, where *n* = 3−10, did not show any phase transitions or other thermal processes by heating up to the melting point (decomposition was observed in the case of DADNB-10, see below). Apparently due to the weaker intermolecular interactions, the compounds with alkyl substituents, DADNB-6 and DADNB-7, have the lowest melting points (Figure 1). DADNB-3 and DADNB-9 have the highest melting temperatures of the neutral compounds. As expected from its

Table 1. Crystallographic Details and Refinement Details

	DADNB-1	DADNB-2-A	DANDB-2-B	DADNB-2-C	DADNB-4	DADNB-5	DADNB-7	DADNB-9	DADNB-10
formula	$C_{10}H_{16}N_6O_4$	$C_{18}H_{14}N_4O_4$	$C_{18}H_{14}N_4O_4$	$C_{18}H_{14}N_4O_4$	$C_{20}H_{18}N_4O_4$	$C_{20}H_{30}N_4O_4$	$C_{12}H_{18}N_4O_4$	$C_{14}H_{24}N_6O_4$	$C_{10}H_{18}Cl_2N_6O_4$
formula weight	284.29	350.33	350.33	350.33	378.38	390.48	282.3	340.39	357.20
temp/K	293(2)	293(2)	293(2)	293(2)	293(2)	293(2)	293(2)	293(2)	293(2)
wavelength/Å	0.71073	0.71073	0.71073	0.71073	0.71073	0.71073	0.71073	0.71073	0.71073
crystal system	orthorhombic	monoclinic	monoclinic	triclinic	triclinic	orthorhombic	monoclinic	monoclinic	monoclinic
space group	*Pbca*	$P2_1/c$	$P2_1/n$	$P\bar{1}$	$P\bar{1}$	*Pnma*	$P2_1/c$	$P2_1/c$	$P2_1/n$
unit cell/(Å, °)	16.138(3)	10.9187(3)	9.2057(2)	7.8650(2)	9.6792(13)	11.6274(11)	8.3647(12)	12.7313(6)	10.3054(3)
	7.0036(12)	10.9859(3)	9.0165(2)	9.6359(2)	10.0246(13)	6.7904(7)	21.533(3)	15.6701(8)	4.43420(10)
	22.750(4)	14.7065(4)	21.1691(5)	23.3040(5)	10.2564(14)	26.582(3)	7.7900(11)	9.4477(4)	32.6413(9)
	90	90	90	89.9010(10)	108.1400(10)	90	90	90	90
	90	109.838(2)	102.4450(10)	88.7770(10)	97.4150(10)	90	92.707(9)	110.8430(10)	97.7700(10)
	90	90	90	70.8770(10)	104.5810(10)	90	90	90	90
volume/Å^3	2571.4(8)	1659.38(8)	1715.82(7)	1668.26(7)	891.7(2)	2098.8(4)	1401.6(3)	1761.48(14)	1477.89(7)
Z	8	4	4	4	2	4	4	4	4
ρ_{calc}/(Mg/m^3)	1.469	1.402	1.356	1.395	1.409	1.236	1.338	1.284	1.596
μ/mm^{-1}	0.116	0.102	0.099	0.102	0.101	0.087	0.102	0.096	0.474
F(000)	1200	728	728	728	396	840	600	728	728
crystal size/mm	0.23, 0.06, 0.05	0.23, 0.09, 0.04	0.41, 0.15, 0.03	0.45, 0.11, 0.08	0.19, 0.09, 0.04	0.34, 0.10, 0.06	0.64, 0.12, 0.03	0.31, 0.22, 0.06	0.30, 0.06, 0.04
θ range/°	6.84−28.86	2.37−28.28	2.46−29.98	0.87−26.02	2.23−27.50	2.89−23.15	2.78−25.07	2.65−26.01	2.52−25.99
index ranges	$-21 \le h \le 21$	$-11 \le h \le 14$	$-12 \le h \le 12$	$-9 \le h \le 6$	$-12 \le h \le 10$	$-12 \le h \le 12$	$-9 \le h \le 9$	$-15 \le h \le 14$	$-12 \le h \le 12$
	$-8 \le k \le 9$	$-14 \le k \le 14$	$-12 \le k \le 12$	$-11 \le k \le 11$	$-11 \le k \le 12$	$-7 \le k \le 7$	$-25 \le k \le 22$	$-19 \le k \le 18$	$-5 \le k \le 5$
	$-30 \le l \le 19$	$-19 \le l \le 19$	$-28 \le l \le 29$	$-28 \le l \le 28$	$-13 \le l \le 13$	$-29 \le l \le 29$	$-9 \le l \le 8$	$-11 \le l \le 11$	$-40 \le l \le 37$
reflections collected	11217	12818	25658	12637	5963	16578	5569	14683	8167
independent reflections	3311 [R(int) = 0.0354]	4067 [R(int) = 0.0236]	4780 [R(int) = 0.0275]	6297 [R(int) = 0.0265]	3915 [R(int) = 0.0114]	1631 [R(int) = 0.0245]	2457 [R(int) = 0.0305]	3422 [R(int) = 0.0265]	2911 [R(int) = 0.0171]
completeness/%	98.10	98.60	95.80	95.70	95.60	99.60	99.20	99.00	99.80
absorption correction	empirical	empirical	empirical	empirical	empirical	empirical	empirical	empirical	empirical
max. and min. transmission	0.9942 and 0.9738	0.9957 and 0.9765	0.9970 and 0.9606	0.9919 and 0.9557	0.9960 and 0.9811	0.9948 and 0.9710	0.9969 and 0.9376	0.9943 and 0.9708	0.9813 and 0.8708
refinement method	FMLS on F^2	FMLS on F^2	FMLS on F^2	FMLS on F^2	FMLS on F^2	FMLS on F^2	FMLS on F^2	FMLS on F^2	FMLS on F^2
data/restraints/parameters	3311/5/201	4067/0/243	4780/0/243	6297/0/485	3915/2/261	1631/22/222	2457/6/191	3422/0/227	2911/1/207
goodness-of-fit on F^2	1.042	1.031	1.046	1.045	1.018	1.061	1.012	1.051	1.055
final R indices [$I > 2\sigma(I)$]	R_1 = 0.0477, wR_2 = 0.1118	R_1 = 0.0477, wR_2 = 0.1140	R_1 = 0.0527, wR_2 = 0.1388	R_1 = 0.0463, wR_2 = 0.1280	R_1 = 0.0562, wR_2 = 0.1499	R_1 = 0.0620, wR_2 = 0.1721	R_1 = 0.0621, wR_2 = 0.1623	R_1 = 0.0557, wR_2 = 0.1567	R_1 = 0.0457, wR_2 = 0.1285
R indices (all data)	R_1 = 0.0743, wR_2 = 0.1258	R_1 = 0.0774, wR_2 = 0.1328	R_1 = 0.0880, wR_2 = 0.1572	R_1 = 0.0800, wR_2 = 0.1532	R_1 = 0.0700, wR_2 = 0.1603	R_1 = 0.0701, wR_2 = 0.1847	R_1 = 0.1203, wR_2 = 0.2001	R_1 = 0.0660, wR_2 = 0.1657	R_1 = 0.0492, wR_2 = 0.1315
largest diff. peak and hole/(e·Å^{-3})	0.222/−0.191	0.183 /−0.186	0.197/−0.199	0.300 /−0.318	0.467 /−0.212	0.217 /−0.273	0.414 /−0.386	0.507 /−0.261	0.650 /−0.456

dx.doi.org/10.1021/jp205793b | *J. Phys. Chem. A* 2011, 115, 10087–10096

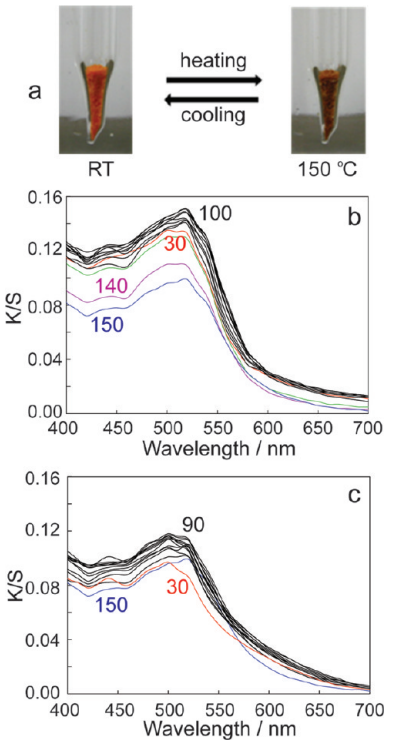

Figure 2. Optical images of DADNB-1 at 30 and 150 °C (a) and UV−visible spectra of DADNB-1 recorded by heating from 30 to 150 °C (b) and subsequent cooling to 30 °C (c). The numbers in the figures are color-coded with the temperatures (in °C) where several characteristic spectra were recorded. Heating and cooling rate: 5 °C/min.

ionic composition, the ammonium salt DADNB-10 was stable to higher temperature (300 °C) relative to the other materials, where it decomposed exothermically (Figure S9). While eight compounds (DADNB-3−DADNBB-10) were not thermochromic, for those having aminoethyl and phenyl substituents, DADNB-1 and DADNB-2, the hot-stage microscopic observations showed that they undergo sharp and reversible color changes, corresponding to effects in their DSC curves. The crystal structures were determined from nine single crystals obtained from seven of these compounds: DADNB-1, DADNB-2 (see below), DADNB-4, DADNB-5, DADNB-7, DADNB-9, and DADNB-10. From DADNB-2, three polymorphs were determined. The relevant crystallographic data are listed in Table 1.

3.2. Thermochromism of DADNB-1. DADNB-1 crystallizes from ethanol as well-shaped orange crystals. When the crystals are heated above RT, they show clearly visible color change from orange-red to brown (Figure 2a). The color change was monitored by reflectance UV−visisble spectroscopy (Figure 2b,c). At RT, the orange form absorbs around 500 nm. Heating to 150 °C results in increased absorption intensity and redshift of the absorption edge, with some increase in the background on the low-energy side. The color change is reversible, and the original orange color is recovered after cooling of the crystals to RT, although the recovery is rather slow.

3.3. Polymorphism and Phase Transitions of DADNB-1. The thermal properties of DADNB-1 were quantified by DSC/TG measurements and IR spectroscopy. As shown in Figure 3, heated DADNB-1 exhibits two endothermic peaks. The first endothermic peak, at 126 °C with ΔH_m = 46 J/g, corresponds to

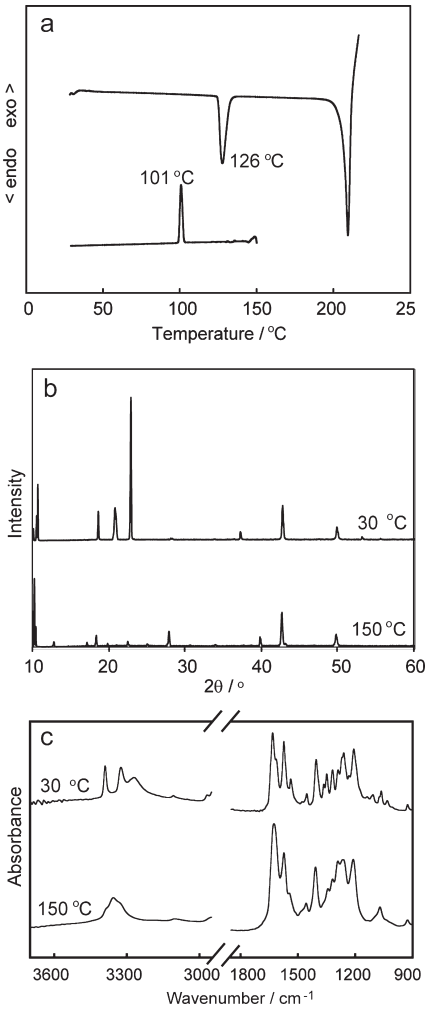

Figure 3. (a) DSC curves recorded by heating and cooling of DADNB-1 at a heating/cooling rate of 10 °C/min. The cooling curve was recorded by cooling from 150 °C after the sample had been heated up to 150 °C. (b) X-ray powder diffraction patterns of DADNB-1 at 30 and 150 °C. (c) The FT-IR spectra of DADNB-1 at 30 and 150 °C.

a phase transition (T_{cc}) of the RT phase (DADNB-1-A) to HT phase (DADNB-1-B; Figure 3a). Comparison with the temperature-resolved UV−visisble spectra showed that this phase transition is associated with the solid-state thermochromism. The second peak is related to melting (T_m). We confirmed by TGA that the sharp increase of exothermic heat flow after the melting is due to sample degradation (Figure S10 in the SI). If the crystals of DADNB-1-B are heated above the phase transition but below the melting/decomposition temperature (150 °C) and subsequently cooled, they undergo a reverse phase transition to DADNB-1-A, a process that is accompanied by an exothermic peak at 101 °C and characterized by ΔH_m = 36 J/g and a 78% recovery of the enthalpy. The characteristic vibrations in the IR spectra of the two phases are assigned in Table 2.

The powder XRD patterns (Figure 3b) confirmed that, although the HT phase DADNB-1-B was crystalline, the two phases have very different crystal structures. In the temperature-resolved IR spectra (Figure 3c), the NH and NH_2 stretching bands of the RT phase at 3328, 3388, and 3270 cm^{-1} were merged above T_{cc} into a single broad band at 3361 cm^{-1}. The intensity of the C═C stretching band of the benzene ring at

dx.doi.org/10.1021/jp205793b |J. Phys. Chem. A 2011, 115, 10087–10096

Table 2. Assignment of the Characteristic Infrared Vibrational Bands of DADNB-1 at 30 and 150 °C

30 °C		150 °C	
wavenumber (cm^{-1})	assignment	wavenumber (cm^{-1})	assignment
3388, 3328	ν(NH)	3361	ν(NH)
3270	$\nu(NH_2)$		$\nu(NH_2)$ ν(OH) from =N−OH
1621	ν(arom.C=C)	1620	ν(arom. C=C)
1572, 1403	$\nu(NO_2)$	1567, 1403	$\nu(NO_2)$

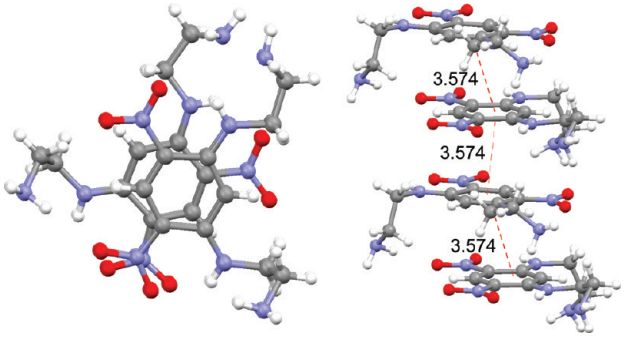

Figure 4. Stacking in the structure of DADNB-1: top view (left) and lateral view (right). The numbers represent the center-to-center distances (in Å).

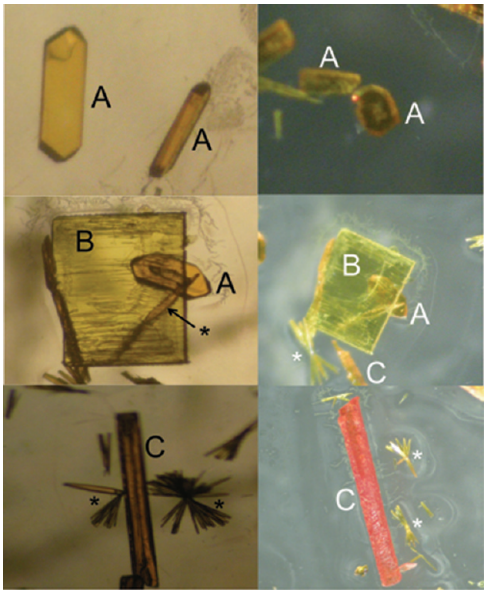

Figure 5. Optical microscopic images, recorded under transmission (left panels) and reflective (right panels) illumination, of different habits of the three polymorphs (A−C) of DADNB-2 that had crystallized concomitantly. The crystals from the impurity (2-chloro-6-phenylamino-3,5-dinitrobenzene) are denoted with asterisks.

1620 cm^{-1} decreased, and the intensity of the NO_2 stretching bands at 1573 and 1403 cm^{-1} decreased. In the structure of the RT phase DADNB-1-A (Figure 4), the equidistant molecules are

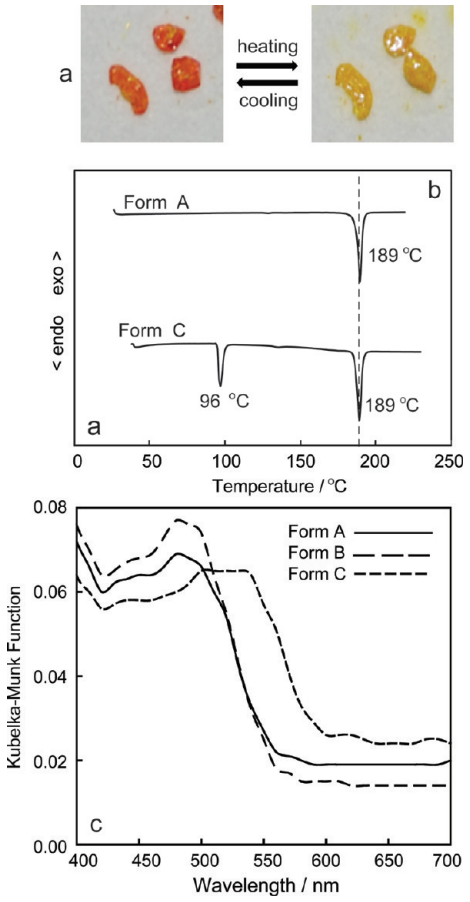

Figure 6. Optical images of crystals of DADNB-2-C recorded at room temperature and at 120 °C (a), DSC curves of forms DADNB-2-A and DADNB-2-C (b), and solid-state reflectance UV−visible spectra of the three forms (c).

displaced and stacked at a center-to-center distance of 3.574 Å. The π-stacking into infinite columns and delocalization of the intramolecular CT along the stacks is responsible for the orange-red coloration of the RT phase. By analogy with BDB3,[8] where the yellow color gradually turns to orange by heating, the deeper red color observed by heating of the RT phase DADNB-1-A, which is also reflected as a gradual red-shift of the absorption edge (Figure 2), can be associated with a gradual increase of the distance of the molecules within the stacks. As in some other cases,[6−8] an intramolecular hydrogen transfer from the amine proton to the nitro-oxygen leading to the nitro-acid form to the nitro group could be, in principle, suggested as possible mechanism of the thermochromic transition of DADNB-1-A to DADNB-1-B, although the validity of such a mechanism remains to be confirmed by direct diffraction methods (see the discussion on the possibility of proton transfer below).

3.4. Polymorphism of DADNB-2. In the course of growing crystals for structure determination of the DADNB-*n* by various methods, we noticed that recrystallization from ethanol of DADNB-2, which contained a small amount of impurity from the nonreacted, monosubstituted precursor 2-chloro-6-phenylamino-3,5-dinitrobenzene, affords batches containing crystals of several different habits and colors. Structure characterization by XRD of many of these crystals (see below) showed that they belong to three distinct polymorphs, denoted here DADNB-2-A, -B,

and -C, that crystallize concomitantly with the crystals from the impurity (Figure 5). The chemical identity of the three forms separated mechanically was confirmed with their ^{1}H NMR spectra in solution (see Figure S11 in the SI). As shown in Figure 5, the crystals of three polymorphs can be readily visually discerned by their habit and color: crystals of DADNB-2-A are dark yellow short prisms, DADNB-2-B crystallizes as thin striated bright yellow square plates, while the crystals of DADNB-2-C are long red prisms. Accordingly, while the absorption of forms A and B peak around 490 nm, form C has an absorption band with a maximum at 550 nm that extends well in the red region, to ~600 nm (Figure 6c). Repeated crystallization experiments showed that different polymorphs of DADNB-2 can be obtained from the crystallization solution in pure form (in the case of DADNB-2-A) or as mixtures, with DADNB-2-A being always the predominant form. The attempt to control the preferred crystallization of the three polymorphs in our hands proved difficult, and it was additionally burdened by the apparent induction effect on the crystallization caused by the impurity. Although we could easily obtain small amount of XRD-quality crystals from all three forms, we were successful in obtaining bulk amount for physicochemical characterization only from DADNB-2-A, which also appears as the thermodynamically most stable form. Additionally, we succeeded in mechanical separation of a very small amount of DADNB-2-C (but not of DADNB-2-B) for DSC analysis. While crystals of forms A and B are stable at RT, the appearance of the crystals of form C changes over time; the apparent mosaicity on the surface of the crystals visibly increases in the course of several days, thus indicating a spontaneous structural transformation.

Table 3. Thermodynamic Properties of Forms A and C of DADNB-2

form	T_{cc} (°C)	ΔH_{cc} (J/g)	T_m (°C)	ΔH_m (J/g)
A			189	78
C	96	43	190	76

3.5. Thermochromism and Phase Transitions of DADNB-2. The thermal properties of the three forms of DADNB-2 were characterized by optical microscopy and, in the case of DADNB-2-A and DADNB-2-C, also with DSC. While heated crystals of DADNB-2-A and DADNB-2-B retained their yellow color, the red crystals of DADNB-2-C underwent a drastic and reversible color change from red to yellow (Figure 6a). This is the first example among the DADNB-type compounds where the low-temperature form absorbs at higher wavelength than the room-temperature form, a thermal analogue to the "negative photochromism" which is observed with some photochromic materials where the absorption of the compound after irradiation is blue-shifted relative to the absorption before the irradiation. The DSC trace (Figure 6b, Table 3) showed two endothermic peaks: the first, at 96 °C, is due to a solid−solid phase transition and is also related to the color change, while the second one (190 °C) is due to melting. The melting point of the HT phase and the respective

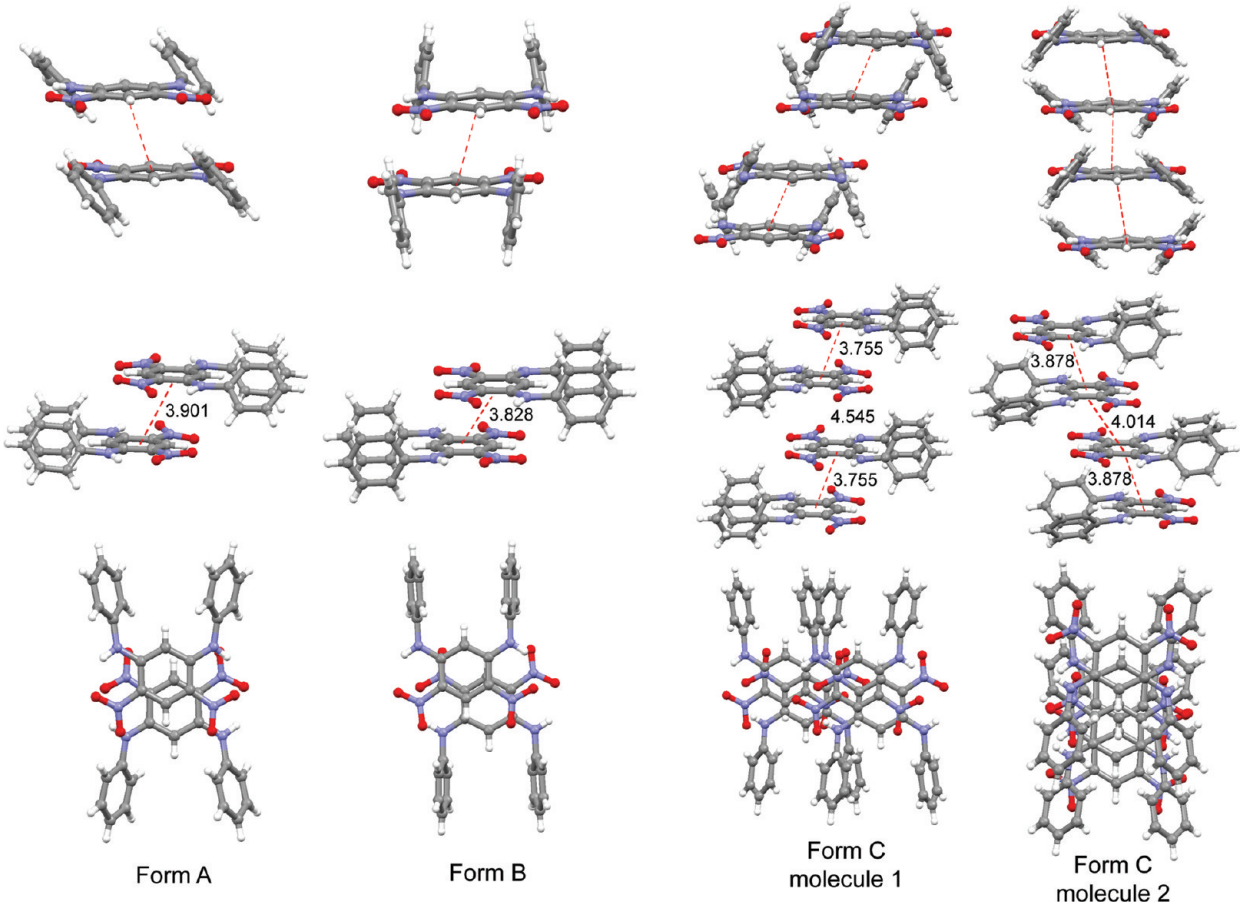

Figure 7. Stacking in the structures of the three polymorphs of DADNB-2: (top) frontal view, (middle) lateral view, and (bottom) top view. The two crystallographically different molecules in phase C are shown. The numbers represent the center-to-center distances (in Å).

enthalpy change are practically identical with those of pure DADNB-2-A (189 °C), indicating that the phase transition that occurs on heating corresponds to transformation of DADNB-2-C to DADNB-2-A. Accordingly, pure DADNB-2-A did not show any thermal effects up to its melting point.

The crystal structures of the three polymorphs of DADNB-2 are shown in Figure 7. The calculated PXRD patterns of the three forms are expectedly different, and the diffraction pattern of the bulk DADNB-2-A conforms to the pattern calculated from the crystal structure (see Figure S12 in the SI). Inspection of the crystal structures of the three polymorphs (Figure 7) unravels the reasons behind the color difference. The only two relevant degrees of freedom in the molecular structure are related to the rotation of the phenyl groups; the nitro groups are constrained by resonance to nearly coplanar disposition with the DADNB moiety. In all structures, the head-to-tail π-stacked arrangement of the DADNB units appears as a persistent supramolecular motif, along with what has been observed previously in the structures of the 1,3-bis(hydroxyalkylamino) homologues.[8] Namely, in the *yellow* forms (A and B), the aromatic chromophores form head-to-tail π-stacked *dimers* that interact through weak $\pi-\pi$ interactions. The center-to-center distances are 3.901 and 3.828 Å in forms A and B, respectively. In the structure of the *red* form (C), on the other hand, the two crystallographic types of chromophores are arranged as two π-stacked *columnar* motifs. The dimers in the first motif, with center-to-center distance of 3.755 Å, and the centroid distance between the neighboring dimers being 4.545 Å, are separated better from each other. In the second motif, the molecules are stacked more uniformly, with an intradimer stacking distance of 3.878 Å and intradimer stacking distance of 4.014 Å. Apparently, the intramolecular CT is strongly influenced by the intermolecular $\pi-\pi$ interactions, along with what was observed with the 1,3-bis(hydroxyalkylamino) analogues.[8] Namely, the in situ HT XRD analysis of BDB3, for instance, evidenced that the *gradual* color change from yellow to red by heating is due to increase of the intradimer and interdimer distances from 3.581 and 3.889 Å to 3.609 and 3.932 Å, respectively. The latter values are comparable to the values 3.878 and 4.014 Å in the second motif of DADNB-2-C, in support of the hypothesis that the red color of this particular phase is due to columnar stacking of the CT chromophores. Additional contribution to the color may arise from the different twist of the phenyl rings, although the fact that both phases A and B are yellow despite the different orientation of the phenyl rings (Figure 7) indicates that this structural feature is not critical for the excited-state energy. The phase transition of the red phase DADNB-2-C to the yellow phase DADNB-2-A, therefore, can be represented as change from columnar structure to a structure composed of isolated dimers of π-stacked molecules. An intuitive mechanism of the structural change induced by heating of DADNB-2-C to the transition temperature would involve gradual increase of the distance between the dimers, to the point when a sudden separation of the dimers from each other occurs, whereupon the structure switches to DADNB-2-A.

3.6. Possibility of Intramolecular Proton Transfer in the DADNB-Type Chromophores. Based on the results described above, it can be concluded that the color change of the two DADNB compounds described here is due to solid−solid phase transitions. In the case of DADNB-2, the DSC of the HT phase strongly evidenced that the transition from red to yellow color is due to a phase change of DADNB-2-C to DADNB-2-A that differ by the packing of the chromophores: by heating, the distance between the head-to-tail stacked molecules in the columns of DADNB-2-C increases until they are separated into molecular dimers at HT (DADNB-2-A). In our previous work,[8] a formation of the aci-nitro form by intramolecular proton transfer was suggested for the compounds BDB*n* in Scheme 1 (n = 2−4) as the mechanism underlying the sharp HT transition from orange to red phase. We have demonstrated there that the origin of this solid−solid phase transition is different from the process responsible for the preceding gradual color change from yellow to orange, because the IR spectral changes are different and the DSC curves showed only the effects characteristic for sharp phase transitions. Because we feel that in the previous report the hypothesis of a thermal proton transfer in BDB*n* compounds was not adequately supported by an appropriate theoretical justification of the feasibility of such process, we elaborate it in more detail here.

The identity of the HT phase in the case of BDB*n* (n = 2−4) as a mononitronic acid, having one of its nitro groups as the aci-nitro tautomer, had been established based on its IR spectral fingerprint (determination of the structure of the HT phases was not feasible due to decreased crystal quality). Although in the 1,2-aminonitrophenyl compounds the aci-nitro group can be normally populated by photoexcitation and proton transfer from the first excited state, as it has been documented by a great number of studies,[14,15] the previous reports have also indicated that a thermal 1,5-proton transfer from the amino group is not a thermally forbidden process. In the absence of an aromatic ring, for the 1,5-proton transfer from an amino group to a nitro group the theoretical calculations predict a barrier of 13.2 kcal/mol. This value is significantly lower than that for proton transfer from a carbon atom (depending on the method and the molecule, the latter has been predicted as 37.8[16] or 41.2[17] and 48.5 kcal/mol[17]), although the process is still costlier in terms of energy relative to a proton transfer from oxygen donor (5.0 kcal/mol).[16] Moreover, the thermal creation of the aci-nitro group is believed to occur even during energetically much less favorable thermal processes, such as the transfer of hydrogen from the methyl group during the pyrolysis of *ortho*-nitrotoluene.[18] At least three factors could decrease this barrier to values accessible by the thermal treatment employed in our previous study (e.g., 127−140 °C) of the three polymorphs of BDB2:

(a) Increased proximity of the amino group and the nitro group due to increased thermal motions at HT with favorable disposition of the nitro group, which is close to planar with the ring. As we demonstrated by HT single crystal XRD,[8] the distance between the proton and the oxygen from the nitro group in BDB2 decreases from 2.019(18) Å at 20 °C to 1.956(19) A at 97 °C, although it should be noted here that the accuracy of parameters which describe such effects are obscured by increased thermal oscillations at HT. Such change is expected to affect the potential energy landscape of the proton by decreasing the width of the double minimum potential and by making the barrier flatter and shallower. Indeed, according to results from calculations on acyclic model system (*cis*-2-nitrovinylamine),[16] the transition state is expected to resemble the product (the aci-nitro form).

(b) Significant decrease of the proton transfer barrier is expected as a result of strong stabilization by intramolecular hydrogen bonding of the product (H-bonded nitronic acid) with the imine nitrogen relative to the intramolecular H-bond of the reactant (H-bonded amino group) with the nitro group. It has already been

demonstrated that both intermolecular[19] and intramolecular[16,20] hydrogen bonds have strong stabilization effect of the aci-nitro form; in fact, intermolecular hydrogen bonding and phenyl substitution can stabilize the aci-nitro group even at RT, which has been evidenced by crystal structure determination.[19]

(c) Due to the presence of a benzene ring, extension of the conjugation of the aci-nitro group attached to the phenylene ring (see Scheme 1) is expected to contribute by an additional decrease of the energy of the nitronic acid relative to the similar equilibrium in an acyclic system. The red-shift of the color of the HT phase in DADNB-1 relative to the RT phase, for instance, seems to be in agreement with such conclusions for an aci-nitro group, which in solution usually absorbs around 410−460 nm.[14,15]

The collective action of the factors (a−c) is expected to make the aci-nitro form in the BDB*n* as well as in the DADNB-1 thermally accessible. Final evidence, however, would require an experiment to produce HT phase of sufficiently high crystallinity to determine its structure. Such experiments are planned in our laboratory for the future.

4. CONCLUSIONS

According to the mechanism suggested for the thermochromism of BDB*n* compounds, the gradual thermochromism is an inherent property of strongly polarized and stacked 1,3-diamino-4,6-dinitrobenzene fragment, which carries the intramolecular CT properties in the structure. Provided that the terminal groups at the alkyl arms are not interfering, by steric or electronic "through-bond" push−pull mechanism with the stacking of the aromatic part, the substituents at the amino groups should be irrelevant to this property. One could then, in principle, conveniently achieve control over the thermochromic activity of similar molecules simply by modifying the terminal groups. The thermochromism could be correspondingly switched on and off by utilizing bulky, nonplanar or strongly electron-active functionalities.

In the 10 new compounds reported here, the hydroxyalkyl arms at the amino groups are symmetrically substituted with a variety of amino-substituents. With two of these materials, those having aminoethyl and phenyl substituents, DADNB-1 and DADNB-2, we observed sharp and reversible color changes in the solid state. Contrary to the BDB*n* compounds (-$(CH_2)_n$OH substitution) and DADNB-1, however, where the IR spectra indicated occurrence of proton transfer, the thermochromic transition of DADNB-2 was spectroscopically characterized as simple structural phase transitions without a chemical change. From DADNB-2 we succeeded to isolate and characterize structurally three polymorphs with different physico-structural properties, for which we established the modes of their interconversion. Notably, contrary to the BDB*n* compounds where the heating results in color change from yellow to red, one of the forms showed a "negative" thermochromism, where the room-temperature form is red and the high-temperature phase is yellow. The current results pave the way for further modification and tuning of the properties of the DADNB-like thermochromic compounds, for instance, by extending the alkyl arms or by modification of the terminal groups. From the viewpoint of the strong intramolecular CT observed with these molecules, particularly in light of its impact on their color, a study of the electrochemistry might be a worthwhile exercise. In continuation of this work, we plan to embark on such experiments.

■ ASSOCIATED CONTENT

Supporting Information. The crystallographic data were deposited within the Cambridge Structural Database under the numbers CCDC 834912−834920. This material is available free of charge via the Internet at http://pubs.acs.org.

■ AUTHOR INFORMATION

Corresponding Author

*Tel.: 81-(0)6-6879-4574 (P.N.); 82-54-478-7685 (S.C.L.). Fax: 81-(0)6-6879-4726 (P.N.); 82-54-478-7710 (S.C.L.). E-mail: pancenaumov@gmail.com (P.N.); leesc@kumoh.ac.kr (S.C.L.).

■ ACKNOWLEDGMENT

This work was supported by the Research Fund, Kumoh National Institute of Technology.

■ REFERENCES

(1) (a) Gage, J. Colour and Culture. *Practice and Meaning from Antiquity to Abstraction*; Thames and Hudson: London, 1993. (b) Gage, J. Colour and Meaning. *Art, Science and Symbolism*; Thames and Hudson: London, 1999. (c) Nassau, K. *The Physics and Chemistry of Color*; Wiley-Interscience: New York, 1983. (d) McDonald, R., Ed. Colour Physics for Industry. *Society of Dyers and Colourists*, 2nd ed.; Bradford: Denver, CO, 1997. (e) Bamfield, P. *Chromic Phenomena*; Royal Society of Chemistry: U.K., 2001.

(2) (a) Ollis, D.; Ormand, K. L.; Sutherland, I. O. *J. Chem. Soc., Chem. Commun* **1968**, 1697. (b) Zerbetto, F.; Monti, S.; Orlandi, G. *J. Chem. Soc., Faraday Trans.* **1984**, *80*, 1513. (c) Makarov, S. P.; Simkin, B. Y.; Minkin, V. I. *Chem. Heterocycl. Compd.* **1988**, 140. (d) Castaldi, G.; Allegrini, P.; Fusco, R.; Longo, L.; Malatesta, V. *J. Chem. Soc., Chem. Commun.* **1991**, 1257. (e) Day, P. N.; Wang, Z. Q.; Rachter, R. *J. Phys. Chem.* **1995**, *99*, 9730. (f) Suh, H.-J.; Lim, W.-T.; Cui, J.-Z.; Lee, H.-S.; Kim, G.-H.; Heo, N.-H.; Kim, S.-H. *Dyes Pigments* **2002**, *57*, 149. (g) Naumov, P.; Yu, P.; Sakurai, K. *J. Phys. Chem. A* **2008**, *112*, 5810.

(3) (a) Cohen, M. D.; Schmidt, G. M. J. *J. Phys. Chem.* **1962**, *56*, 2442. (b) Cohen, M. D.; Schmidt, B.; Flavian, S. *J. Chem. Soc.* **1964**, 2041. (c) Ledbetter, J. W. *J. Phys. Chem.* **1977**, *81*, 54. (d) Hoshino, N.; Inabe, T.; Mitani, T.; Maruyama, Y. *Bull. Chem. Soc. Jpn.* **1988**, *61*, 4207. (e) Inabe, T.; Gautier-Luneau, I.; Hoshino, N.; Okaniwa, K.; Okamoto, H.; Mitani, T.; Nagashima, U.; Maruyama, Y. *Bull. Chem. Soc. Jpn.* **1991**, *64*, 801. (f) Takase, A.; Sakagami, S.; Nonaka, K.; Koga, T. *J. Raman Spectrosc.* **1993**, *24*, 447. (g) Johmoto, K.; Sekine, A.; Uekusa, H.; Ohashi, Y. *Bull. Chem. Soc. Jpn.* **2009**, *82*, 50. (h) Sliwa, M.; Spangenberg, A.; Malfant, I.; Lacroix, P. G.; Métivier, R.; Pansu, R. B.; Nakatani, K. *Chem. Mater.* **2008**, *20*, 4062. (i) Sliwa, M.; Mouton, N.; Ruckebusch, C.; Aloïse, S.; Poizat, O.; Buntinx, G.; Métivier, R.; Nakatani, K.; Masuhara, H.; Asahi, T. *J. Phys. Chem. C* **2009**, *113*, 11959. (j) Sliwa, M.; Naumov, P.; Choi, H.-J.; Nguyen, Q.-T.; Debus, B.; Delbaere, S.; Ruckebusch, C. *ChemPhysChem* **2011**, *12*, 1669.

(4) (a) Agranat, I.; Tapuhi, Y. *J. Org. Chem.* **1979**, *44*, 1941. (b) Tapuhi, Y.; Kalisky, O.; Agranat, I. *J. Org. Chem.* **1979**, *44*, 1949. (c) Stezowski, J. J.; Biedermann, P. U.; Hildenbrand, T.; Dorsch, J. A.; Eckhardt, C. J.; Agranat, I. *J. Chem. Soc., Chem. Commun.* **1993**, 213. (d) Pogodin, S.; Rae, I. D.; Agranat, I. *Eur. J. Org. Chem.* **2006**, 5095. (e) Levy, A.; Pogodin, S.; Cohen, S.; Agranat, I. *Eur. J. Org. Chem.* **2007**, 5198. (f) Pogodin, S.; Suissa, M. R.; Levy, A.; Cohen, S.; Agranat, I. *Eur. J. Org. Chem.* **2008**, 2887. (g) Biedermann, P. U.; Stezowski, J. J.; Agranat, I. *Chem.—Eur. J.* **2006**, *12*, 3345. (h) Nielsen, W. G.; Fraenkel, G. K. *J. Chem. Phys.* **1953**, *21*, 1619. (i) Theilacker, W.; Kortüm, G.; Elliehausen, W. H. *Z. Naturforsch.* **1954**, *B9*, 167. (j) Theilacker, W.; Kortüm, G.; Elliehausen, W. H. *Chem. Ber.* **1956**, *89*, 1578. (k) Mills, J. F. D.; Nyburg, S. C. *J. Chem. Soc.* **1963**, 308. (l) Schönberg, A.; Mustafa, A.; Sobhy, M. E. E.-D. *J. Am. Chem. Soc.* **1953**, *75*, 3377.

(m) Naumov, P.; Ishizawa, N.; Wang, J.; Pejov, Lj.; Pumera, M.; Lee, S. C. *J. Phys. Chem. A* **2011**, doi: 10.1021/jp2040339.

(5) (a) Day, J. H. *Chem. Rev.* **1963**, *63*, 65. (b) Tansienhee, L.; Lavabre, D.; Levy, G.; Micheau, J. C. *New J. Chem.* **1989**, *13*, 227. (c) White, M. A.; LeBlanc, M. *J. Chem. Educ.* **1999**, *76*, 1201. (d) Buklevski, M.; Petruševski, V. *J. Chem. Educ.* **2009**, *86*, 30. (e) Changyun, C.; Zhihua, Z.; Yiming, Z.; Jiangyan, D. *J. Chem. Educ.* **2000**, *77*, 1206. (f) Van Oort, M. J. M. *J. Chem. Educ.* **1988**, *65*, 84. (g) Choi, S.; Larrabee, J. A. *J. Chem. Educ.* **1989**, *66*, 774. (h) Hughes, J. G. *J. Chem. Educ.* **1998**, *75*, 57. (h) Kinuta, T.; Sato, T.; Tajima, N.; Kuroda, R.; Matsubara, Y.; Imai, Y. *J. Mol. Struct.* **2010**, *982*, 45.

(6) Lee, S. C.; Jeong, Y. G.; Jo, W. H.; Kim, H.-J.; Jang, J.; Park, K.-M.; Chung, I. H. *J. Mol. Struct.* **2006**, *825*, 70.

(7) Lee, S. C.; Jeong, Y. G.; Jang, S. H.; Jo, W. H. *Fib. Polym.* **2007**, *8*, 234.

(8) Naumov, P.; Lee, S. C.; Ishizawa, N.; Jeong, Y. G.; Chung, I. H.; Fukuzumi, S. *J. Phys. Chem. A* **2009**, *113*, 11354.

(9) (a) Threlfall, T. J. *Analyst* **1995**, *120*, 2435.(b) Bernstein, J. *Polymorphism in Molecular Crystals*; Oxford University Press: Oxford, 2002. (c) Bernstein, J. *Cryst. Growth Des.* **2011**, *11*, 632.

(10) *APEX2* (ver. 2.1−4) and *SAINT* (ver. 7.34A); Bruker AXS, Inc.: Madison, WI, 2007.

(11) Sheldrick, G. M. *SADABS*; University of Göttingen: Göttingen, Germany, 1996.

(12) (a) Sheldrick, G. M. *Acta Crystallogr., Sect. A* **2008**, *64*, 112. (b) Altomare, A.; Cascarano, G.; Giacovazzo, C.; Guagliardi, A.; Burla, M. C.; Polidori, G.; Camalli, M. J. *Appl. Crystallogr.* **1994**, *27*, 435.

(13) Sheldrick, G. M. E. *SHELXL-97*; University of Göttingen: Göttingen, Germany, 1997.

(14) (a) Scherl, M.; Haarer, D.; Fischer, J.; DeCian, A.; Lehn, J.-M.; Eichen, Y. *J. Phys. Chem.* **1996**, *100*, 16175. (b) Casalegno, R.; Corval, A.; Kuldova, K.; Ziane, O.; Trommsdorff, H. P. *J. Lumin.* **1997**, *72*−*74*, 78. (c) Ziane, O.; Casalegno, R.; Corval, A. *Chem. Phys.* **1999**, *250*, 199. (d) Shinohara, S.; Takeda, J.; Ooike, T.; Kurita, S. *J. Phys. Soc. Jpn.* **1999**, *68*, 1725. (e) Schworer, M.; Wirz, J. *Helv. Chim. Acta* **2001**, *84*, 1441. (f) Corval, A.; Casalegno, R.; Ziane, O.; Burrows, H. D. *J. Phys. Chem. A* **2002**, *106*, 4272. (g) Naumov, P. *Bull. Chem. Technol. Macedonia* **2004**, *23*, 87. (i) Naumov, P. *J. Mol. Struct.* **2006**, *783*, 1. (h) Matveev, M .R.; Khokhlachev, V. O.; Ponyaev, A. I. *Russ. J. Gen. Chem.* **2006**, *76*, 1319. (i) Khokhalachev, V. O.; Ponyaev, A. I. *Russ. J. Gen. Chem.* **2007**, *77*, 1406. (j) Zakhs, E. R.; El'tsov; Liashenko, E. V. *Zh. Org. Khim.* **1978**, *9*, 1992. (k) Ponyaev, A. I.; Ol'khovskii, V. V.; Zakhs, E. R.; El'tsov, A. V. *Zh. Org. Khim.* **1986**, *22*, 2217. (l) El'tsov, A. V.; Zakhs, E. R.; Ponayev, A. I.; Frolova, T. I. *Zh. Org. Khim.* **1978**, *8*, 1760. (m) Zakhs, E. R.; Ponyaev, A. I.; Subotina, M. A.; El'tsov, A. V. *Zh. Obsch. Khim.* **2001**, *71*, 1142. (n) El'tsov, A. V.; Zakhs, E R.; Frolova, T I. *Zh. Obsch. Khim.* **1976**, *5*, 1088. (o) Zakhs, E. R.; Ponyaev, A. I.; Sergeev, A. M.; Frolova, T. I.; El'tsov, A. V. *Zh. Org. Khim.* **1979**, *15*, 2129. (p) Ponyaev, A. I.; Frolova., T. I.; Zakhs, E. R.; El'tsov, A V. *Zh. Org. Khim.* **1977**, *7*, 1548. (q) El'tsov, A. V.; Zakhs, E. R.; Ponyaev, A I. *Zh. Org. Khim.* **1980**, *10*, 2176. (r) Goeschen, C.; Herges, R.; Richter, J.; Tokarczyk, B.; Wirz, J. *Helv. Chim. Acta* **2009**, *92*, 1909. (s) Nagaya, M.; Kudoh, S.; Nakata, M. *Chem. Phys. Lett.* **2006**, *427*, 67.

(15) Lammertsma, K.; Bharatam, P. V. *J. Org. Chem.* **2000**, *65*, 4662.

(16) Il'ichev, Y. V.; Wirz, J. *J. Phys. Chem. A* **2000**, *104*, 7856.

(17) He, Y. Z.; Cui, J. P.; Mallard, W. G.; Tsang, W. *J. Am. Chem. Soc.* **1988**, *110*, 3754.

(18) Bock, H.; Dieneli, R.; Schodel, H.; Havlas, Z; Herdtweck, E.; Herrmann, W. A. *Angew. Chem., Int. Ed.* **1993**, *32*, 1758.

(19) Kang, F.-A.; Yin, C.-L.; She, S.-W. *J. Org. Chem.* **1996**, *61*, 5523.

(20) Matveev, M. R.; Ponyaev, A. I.; El'tsov, A. V. *Russ. J. Gen. Chem.* **2001**, *71*, 1286.